Restricted inactivation of serum response factor to the cardiovascular system

Joseph M. Miano*†‡, Narendrakumar Ramanan†§, Mary A. Georger*, Karen L. de Mesy Bentley¶, Rachael L. Emerson*, Robert O. Balza, Jr.‖, Qi Xiao‖, Hartmut Weiler**, David D. Ginty§††, and Ravi P. Misra‡‖

*Center for Cardiovascular Research, Aab Institute of Biomedical Sciences, ¶Electron Microscope Research Core, School of Medicine, University of Rochester, 601 Elmwood Avenue, Rochester, NY 14642; §Department of Neuroscience, Howard Hughes Medical Institute, School of Medicine, Johns Hopkins University, Baltimore, MD 21205; and ‖Department of Biochemistry, Medical College of Wisconsin and **Blood Research Institute, 8701 Watertown Plank Road, Milwaukee, WI 53226

Edited by Eric N. Olson, University of Texas Southwestern Medical Center, Dallas, TX, and approved October 18, 2004 (received for review August 16, 2004)

Serum response factor (SRF) directs programs of gene expression linked to growth and muscle differentiation. To investigate the role of SRF in cardiovascular development, we generated mice in which SRF is knocked out in >80% of cardiomyocytes and >50% of vascular smooth muscle cells (SMC) through SM22α-Cre-mediated excision of SRF's promoter and first exon. Mutant mice display vascular patterning, cardiac looping, and SRF-dependent gene expression through embryonic day (e)9.5. At e10.5, attenuation in cardiac trabeculation and compact layer expansion is noted, with an attendant decrease in vascular SMC recruitment to the dorsal aorta. Ultrastructurally, cardiac sarcomeres and Z disks are highly disorganized in mutant embryos. Moreover, SRF mutant mice exhibit vascular SMC lacking organizing actin/intermediate filament bundles. These structural defects in the heart and vasculature coincide with decreases in SRF-dependent gene expression, such that by e11.5, when mutant embryos succumb to death, no SRF-dependent mRNA expression is evident. These results suggest a vital role for SRF in contractile/cytoskeletal architecture necessary for the proper assembly and function of cardiomyocytes and vascular SMC.

Cre recombinase | knockout | myocardin | SM22α

Serum response factor (SRF) is a widely expressed transcription factor that orchestrates disparate programs of gene expression through a 1,216-fold degenerate element known as a CArG box. One or more CArG boxes (consensus = $CC(W_6)GG$) are found within the proximal promoter or first intron of >60 SRF-dependent genes, half of which are restricted to cardiac, skeletal, and smooth muscle (SM) cells (SMCs) (1, 2). Genetic inactivation of SRF in amoeba (3), worm (4), fly (5), and mouse embryonic stem cells (6) has confirmed a critical role for SRF in normal cytoskeletal architecture, cell adhesion, cell migration, and/or animal movement. These results are consistent with data in transgenic reporter mice showing the functional importance of CArG elements in muscle promoter activity (2, 7).

Because many of the SRF-dependent genes in mammals are associated with cellular locomotion, it is anticipated that inactivation of SRF will lead to loss in both CArG-dependent muscle gene expression and normal contractile activity. However, SRF null mice die well before the emergence of muscle cells, precluding an evaluation of this thesis (8). Here, we show that cardiac/SMC-restricted inactivation of SRF results in embryonic lethality at approximately embryonic day (e)11.5 days. Mutant mice display severe defects in cardiac trabeculation and sarcomeric assembly as well as altered SMC recruitment to the dorsal aorta and the absence of SMC actin/intermediate filament bundles. The structural defects in cardiomyocytes and SMC precede the loss of SRF-dependent gene expression in these cells. Thus, SRF controls events associated with proper assembly of cytoskeletal/contractile elements and terminal muscle differentiation. As this work was completed, Parlakian *et al.* (9) reported a heart-specific knockout of SRF with similar defects in cardiac trabeculation.

Materials and Methods

Generation of SRF$^{f/f}$ and SM22α-Cre Mice. *LoxP* sites were inserted 1,400 bp upstream and 1,135 bp downstream of the transcription start site, resulting in a floxed 5′ promoter and exon 1. As depicted in Fig. 1, excision of the floxed SRF allele results in removal of key regulatory elements shown to be important for SRF promoter activity *in vitro* and *in vivo* (10, 11). In addition, many of the DNA-binding and dimerization residues of SRF are excised upon Cre recombination. As predicted, both expression and DNA-binding activity of SRF are essentially abrogated in neonatal cardiomyocytes null for SRF (Fig. 7, which is published as supporting information on the PNAS web site). A more detailed description of the targeting allele will be published elsewhere (N.R. and D.D.G., unpublished work). A 1.4-kb *Eco*RI/*Sal*I fragment of the mouse SM22α promoter was fused to Cre recombinase and CD-1 transgenic mice generated in the Medical College of Wisconsin's Core Facility. Activity of SM22α-Cre was ascertained with the ROSA26 reporter line (R26R), as described (12). Homozygous floxed SRF (SRF$^{f/f}$) mice (bred on a CD-1 background) were crossed with SRF$^{f/+}$/SM22Cre$^{+/-}$ mice to generate SRF$^{f/f}$/SM22Cre$^{+/-}$ mice at the expected frequency of 25%, which was seen through e11.5; no viable embryos were seen after e11.5. For the studies reported here, we examined a total of 22 mutants and 26 wild-type embryos from e8.5 through e11.5.

Histology, Immunohistochemistry, and *in Situ* Hybridization. Staged embryos were fixed in 4% paraformaldehyde and embedded in paraffin for all histological assays. Embryos were cut at 4 μm and stained with hematoxylin/eosin for general morphology. Adjacent sections were processed for *in situ* hybridization (ISH) or immunohistochemistry. Antibodies to SRF (Santa Cruz Biotechnology, sc-335) and SMα actin (SMA) (Dako, Carpinteria, CA; M0851) were used at dilutions of 1:1,200 and 1:1,000, respectively. Universal secondary antisera (1:400) and horseradish peroxidase were from Richard-Allan Scientific (Kalamazoo, MI) (R50H). ISH was carried out as described with riboprobes to SMC markers (13) and cardiac markers (kind gift of Gary Lyons, University of Wisconsin, Madison). Images were acquired with an Olympus (Melville, NY) digital camera and processed in PHOTOSHOP (Adobe Systems, San Jose, CA). All

This paper was submitted directly (Track II) to the PNAS office.

Abbreviations: SRF, serum response factor; SM, smooth muscle; SMC, SM cell(s); ISH, *in situ* hybridization; R26R, ROSA26 reporter; *en*, embryonic day *n*; SMA, SMα actin.

†J.M.M. and N.R. contributed equally to this work.

‡To whom correspondence may be addressed. E-mail: j.m.miano@rochester.edu or rmisra@mcw.edu.

‡‡To whom requests for SRF floxed mice should be addressed.

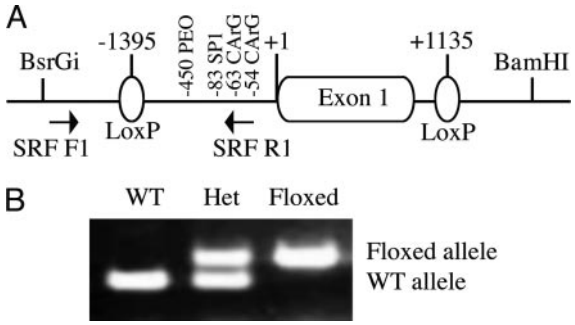

Fig. 1. Floxed SRF targeting allele. (*A*) Schematic of SRF targeting allele and position of loxP sites upstream of promoter and downstream of exon 1. Regulatory elements in proximal promoter are indicated. (*B*) PCR genotyping depicting wild-type allele vs. heterozygous and homozygous floxed alleles.

quantitative measures, were carried out by two independent observers and the data analyzed in PRISM (GraphPad, San Diego). For two measures, an unpaired *t* test was used, and for multiple measures, a one- or two-way ANOVA with Bonferroni post hoc testing was done.

RT-PCR Assay. Total RNA was isolated from microdissected e10.75 mouse hearts by using the Qiagen RNAeasy kit (Qiagen, Valencia, CA). RNA was reverse-transcribed by using random hexamer primers and MMLV RTase (Roche, Indianapolis) at 42°C for 30 min. Radioactive-labeled reactions were performed within each primer pair's linear range of amplification and the data quantitated with a PhosphorImager. Mutant signals were normalized to their corresponding GAPDH control and the ratios expressed as fold changes from wild-type controls. Specific PCR conditions and primer set sequences are available upon request.

Electron Microscopy. e10.5 embryos were fixed in 2.5% glutaraldehyde, postfixed in 1% osmium tetroxide, dehydrated, and embedded in Epon/Araldite resin. Thin sections (70 nm) were placed onto Formvar-coated slot grids and stained with uranyl acetate and lead citrate. Grids were examined with a Hitachi (Tokyo) 7100 electron microscope and images captured by using a Megaview III digital camera (Soft Imaging System, Lakewood, CO).

Results

Activity of SM22α-Cre in R26R Mice. To ascertain when SM22α-driven Cre activity is manifested during development, we crossed our SM22α-Cre line with the R26R reporter mouse line (12). SM22α-Cre activity first emerges in the embryonic heart at e8.5 (Fig. 2*A*). Thereafter, Cre activity is observed in the dorsal aorta, umbilical vessels, and throughout the atrial and ventricular myocardium (Fig. 2 *B–D)*. These results are similar to data reported previously with a conventional SM22α promoter-driven lacZ transgene (14, 15), with the exception that there is promoter activity in both ventricles and some minor activity in the head and tail region (Fig. 2 *B* and *D*). Together, these data indicate that our SM22α-Cre mouse should restrict the inactivation of SRF and other floxed alleles to the cardiovascular system.

Efficiency of SRF Inactivation in Developing Heart and Aorta. $SRF^{f/f}$ mice were crossed with $SRF^{f/+}/SM22\alpha Cre^{+/-}$ to generate $SRF^{f/f}/SM22\alpha Cre^{+/-}$ mice (hereafter referred as mutants). All studies reported here compare mutants with $SRF^{f/+}/SM22\alpha Cre^{+/-}$ (hereafter abbreviated as wild-type). There were no differences in any of the parameters assayed among the various nonmutant

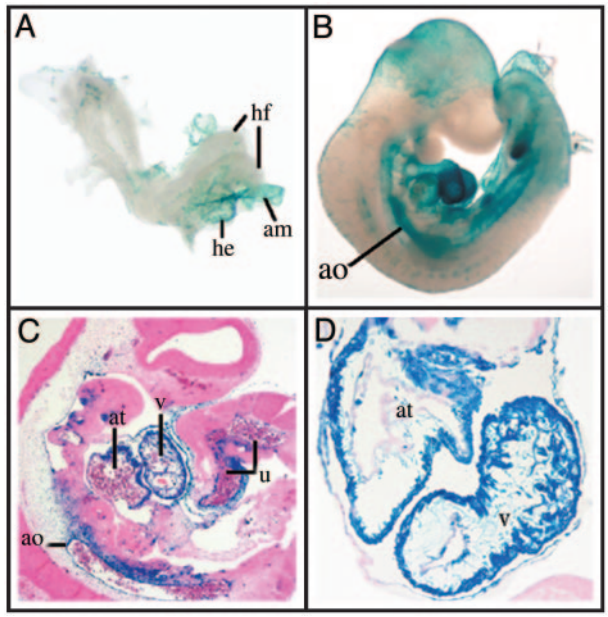

Fig. 2. SM22α-Cre activity in the R26R mouse. Mice carrying both the R26R and SM22α-Cre alleles stained for lacZ at e8.5 (*A*) and e10.5 (*B–D*). The blue staining in the indicated structures reflects β-galactosidase activity due to Cre-mediated excision of a floxed PGK neo cassette upstream of the *lacZ* gene within the ROSA26 locus (12). am, amnion; ao, aorta; at, atrium; he, heart; hf, head folds; v, ventricle; u, umbilical vessels.

mouse lines ($SRF^{f/+}$, $SRF^{f/f}$, and $SRF^{f/+}/SM22\alpha Cre^{+/-}$; data not shown). Consistent with previous mRNA studies (16), SRF protein is expressed abundantly in cardiomyocytes and subjacent SMC of the dorsal aorta in wild-type embryos (Fig. 3 *C*, *E*, and *G*). Mutant mice display decreases in SRF protein in both muscle types (Fig. 3 *D*, *F*, and *H)*. Rigorous quantitation reveals ≈50% of cardiomyocytes staining positive for SRF in both wild-type and mutant hearts at e8.5 (Fig. 3*I*). Whereas the number of wild-type cardiomyocytes positive for SRF increases to >80% between e9.5 and e11.5, a progressive and statistically significant decrease in SRF protein is observed in mutant cardiomyocytes over this time span (Fig. 3*I)*. A 59% decrease in SRF protein is noted in e10.5 mutant vascular SMC immediately subjacent to endothelial cells of the dorsal aorta (Fig. 3*J*). Comparable SRF immunostaining is seen in the central nervous system, developing gut, liver, pharyngeal arches, endothelium, and endocardium of mutant and wild-type embryos (data not shown). These results demonstrate that the SM22α-Cre transgene is effective in restricting the inactivation of SRF to cardiomyocytes and vascular SMC of the cardiovascular system.

SRF Mutant Mice Display Growth Retardation and Cardiovascular Defects. As expected from SRF protein data (Fig. 3*I*), no discernable changes in the heart and vasculature are detected at e8.5 (data not shown). However, growth of mutant mice is severely compromised at e10.5 (Fig. 3 *A* vs. *B*). Wild-type mice display prominent cardiac trabeculations and a normal compact zone at this time point (Fig. 3 *C* and *E)*. In contrast, mutants show poorly developed trabeculations and a thinning of the compact zone (Fig. 3 *D* and *F*). Some mutant embryos present with pericardial effusion and hemorrhage (data not shown). Consistent with a previous report (9), these histological changes are not associated with any change in cardiomyocyte proliferation or apoptosis at e10.5 (data not shown; Fig. 8, which is published as supporting information on the PNAS web site). However, 1 day later, mutant embryos display elevated apoptosis

DEVELOPMENTAL BIOLOGY

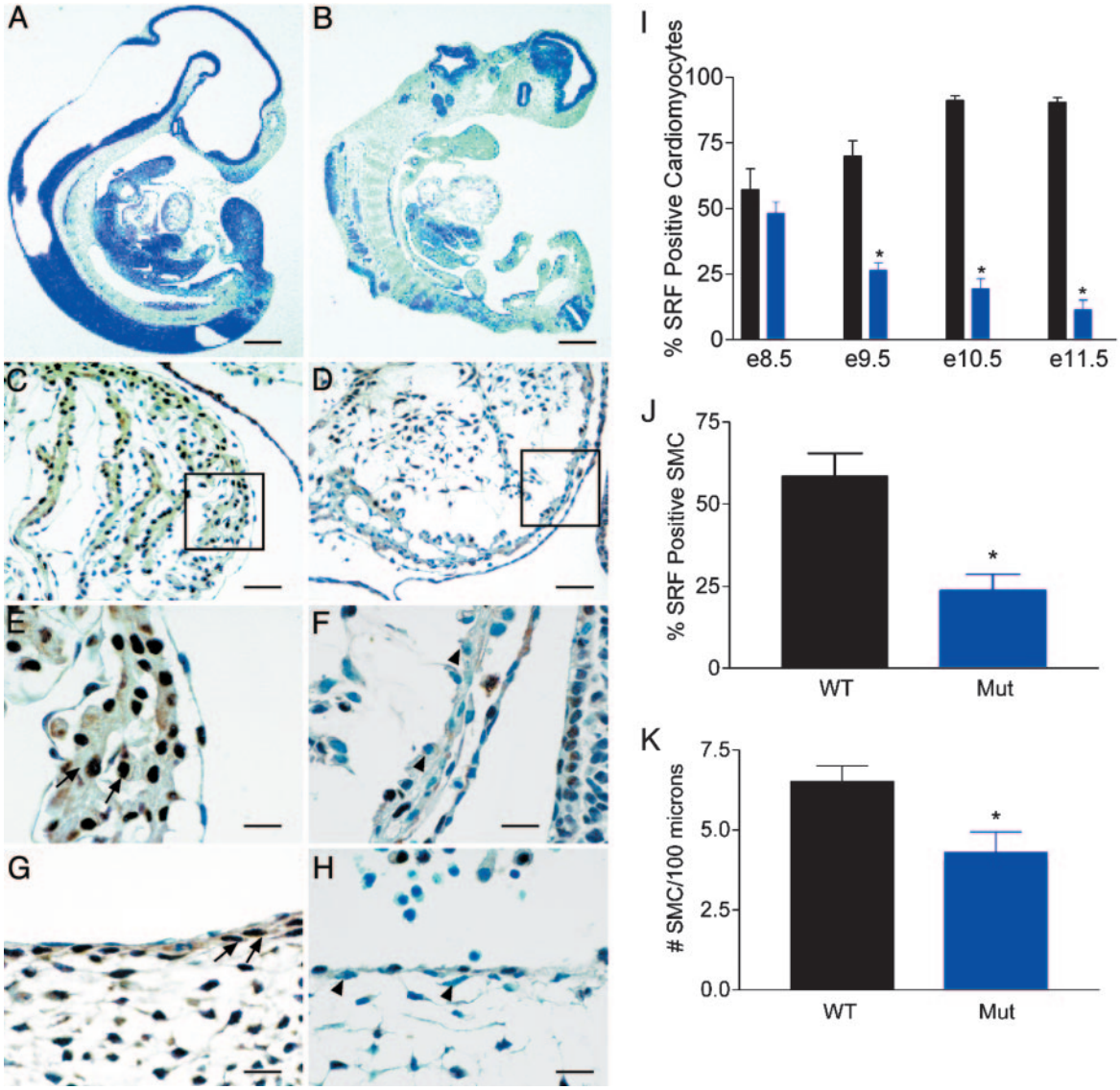

Fig. 3. Cardiac/vascular morphology and SRF expression in wild-type vs. mutant embryos. Hematoxylin/eosin-stained wild-type (*A*) and mutant (*B*) e10.5 embryos are shown. (Bars, 400 μm.) SRF immunostaining of wild-type (*C* and *E*) and mutant (*D* and *F*) hearts shows marked differences in levels of SRF (brown nuclei) as well as cardiac trabeculation and compact zone thickness. (Bars, 30 μm.) *E* and *F* represent magnified images of the boxes in *C* and *D*, respectively. (Bars, 10 μm.) The dorsal aorta of wild-type mice shows greater accumulation of SRF-stained aortic SMC (*G*) than in mutants (*H*). (Bars, 10 μm.) Arrows indicate SRF positive cardiomyocytes (*E*) or SMC (*G*) in wild types, and arrowheads point to SRF-negative cardiomyocytes (*F*) and SMC (*H*) in mutants. *I* shows the percent SRF immunoreactivity in ventricular cardiomyocytes; $n = 3$–5 e10.5 embryos per time point. Beginning at e9.5, the difference between wild-type (black bars) and mutant (blue bars) cardiomyocyte SRF expression was statistically significant (asterisks here and below denote $P < 0.05$). *J* summarizes similarly quantitated SRF immunoreactive staining in subjacent SMC of the dorsal aorta; $n = 3$ e10.5 embryos per condition. *K* shows the number of SMC immediately subjacent to the endothelium per 100 μm of dorsal aorta; $n = 3$ e10.5 embryos per condition.

in the heart and throughout the embryo proper (data not shown and Fig. 8).

The most prominent phenotype in the dorsal aorta of mutant mice is a diminution in the number of subjacent SMC at the dorsal edge of the aorta, the majority of which display no detectable SRF expression (Fig. 3 *G* vs. *H*). We calculate ≈35% decrease in the number of presumptive SMC at the dorsal aspect of the aorta (Fig. 3*K*). Consistent with the absence of SM22α promoter activity in endothelial cells (14, 15), we see no changes in vascular patterning of mutant embryos. Thus, SM22α-Cre-mediated excision of SRF results in selective perturbations of the developing heart and aortic vessel wall.

Ultrastructural Defects in e10.5 SRF Mutant Mice. The hearts of e10.5 wild-type and mutant mice show little evidence of apoptosis and display normal mitochondrial number and morphology as well as gap junctions at intercalated disks (data not shown). In wild-type mice, cardiac sarcomere structure is evident with normal periodicity of Z disks (Fig. 4*A*). Wild-type sarcomeres often appear in tandem through Z disk connections, and myofilaments are arrayed parallel to one another across the sarcomere (Fig. 4*B*). Mutants, however, present with disorganized sarcomeres and Z disks that are not assembled properly into repeating units (Fig. 4*C* and Fig. 9, which is published as supporting information on the PNAS web site). Consequently, myofilaments appear in disarray and often end blindly, with little evidence of Z disk association (Fig. 4*D*).

Wild-type vascular SMCs begin to accumulate at the dorsal aspect of the aorta with zones of actin/intermediate filament bundles near the plasma membrane (Fig. 4 *E* and *F*) and in

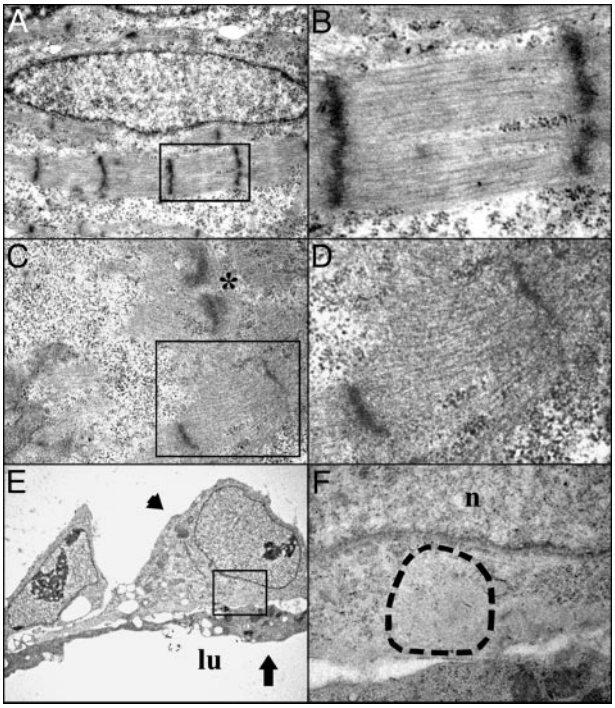

Fig. 4. Electron microscopy of e10.5 hearts. (*A*) Wild-type cardiac sarcomeres show periodic units of myofilaments delineated by Z disks (×10,000). (*B*) Higher magnification of boxed area in *A* demonstrating normal parallel arrangement of myofilaments and normal Z disk structure (×30,000). (*C*) Mutant cardiac sarcomeres with marked disorganization of myofilaments and distorted Z disks (asterisk) (×15,000). (*D*) Higher magnification of boxed area in *C* demonstrating an abnormal sarcomere with disorganized myofilaments and aberrant Z disks (×30,000). (*E*) Wild-type dorsal aortic SMC (arrowhead) immediately subjacent to endothelium (arrow) (×4,000). lu, lumen. (*F*) Higher magnification of boxed area in *E* illustrating a zone of actin/intermediate filaments (dashed circle). n, nucleus. These zones of thin filaments are free of any organelles and are often found near the plasma membrane of SMC (×20,000). Mutant SMC did not contain such zones of filament bundles (see text).

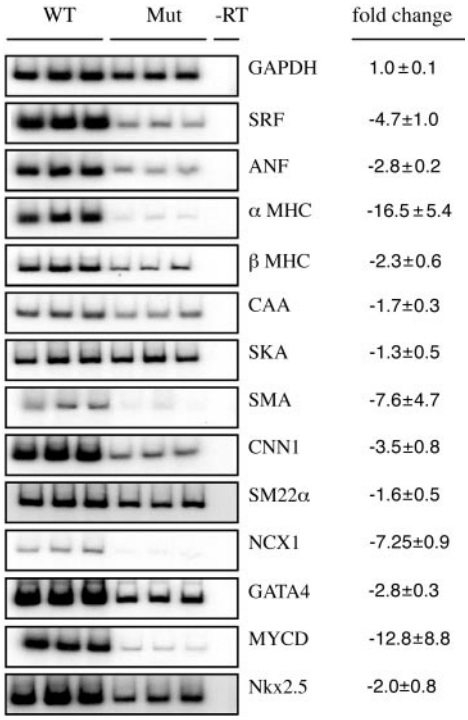

Fig. 5. RNA expression of cardiac/SMC markers. Semiquantitative RT-PCR analysis was performed on total RNA from individual hearts ($n = 3$) of e10.75 wild-type (WT) or mutant (Mut) embryos. Each lane represents 28 cycles of PCR from one individual heart sample demonstrated to be within the linear range of amplification (data not shown). α-^{32}P-labeled PCR products were quantitated (see *Materials and Methods*), and the fold change is given as the mean of three measurements ± SD. ANF, atrial natriuretic factor; α MHC, α myosin heavy chain; β MHC, β myosin heavy chain; CAA, cardiac α actin; SKA, skeletal α actin, CNN1, SM calponin; NCX1, cardiac sodium–calcium exchanger; MYCD, myocardin.

lamellipodia (Fig. 10, which is published as supporting information on the PNAS web site). No SMC actin/intermediate bundles are evident in SRF mutants (Fig. 10). Thus, inactivation of SRF in cardiomyocytes and SMC leads to ultrastructural defects in contractile/cytoskeletal assembly.

SRF-Dependent Gene Expression Is Compromised in Mutant Embryos. We performed radiolabeled RT-PCR to assess expression of endogenous SRF-dependent genes in e10.75 hearts. As expected from our protein data (Fig. 3), SRF mRNA decreases, but is not completely abolished, in the hearts of mutants, with a corresponding decrease in most known SRF-dependent genes (e.g., SMA and NCX1). Interestingly, skeletal α actin, reportedly SRF-dependent, shows little change in expression at this time point. This is consistent with data seen in neonatal cardiomyocytes lacking SRF (R.O.B. and R.P.M., unpublished work), suggesting that alternative SRF-independent pathways may regulate this and possibly other genes. We also observe decreases in several cardiovascular transcription factors (bottom three blots in Fig. 5). We attribute the different levels of down-regulation across SRF-dependent genes to varying mRNA half-lives and redundancies in the transcriptional regulation of each gene's promoter.

To evaluate the *in vivo* expression of SRF-dependent genes more closely, we performed ISH. Little change in SRF-dependent gene transcription is detected by ISH at e8.5–e9.5 (data not shown). However, consistent with RT-PCR data, we see decreases in SMA in the mutant heart at e10.5 (Fig. 6*J*). A similar decrease in SMA is noted in the dorsal aorta of e10.5 mutants (Fig. 6*J*). Transcripts to cardiac α actin (Fig. 6*B*), SM22α (Fig. 6*F*), and atrial natriuretic factor (Fig. 11, which is published as supporting information on the PNAS web site) are also reduced in the cardiovascular system of e10.5 mutant embryos. By e11.5, no detectable mRNA expression of SRF-dependent genes is observed in the heart or dorsal aorta (Fig. 6 *D*, *H*, and *L*). Of interest, however, we consistently see persistent expression of SMA protein in both the heart and aorta of e11.5 mutants (Fig. 6*P*). We have also looked at more definitive markers of SMC differentiation (SM-calponin and SM myosin heavy chain) and find these to be totally absent from the dorsal aorta of e11.5 mutants (data not shown). Together, these results provide genetic proof for the dependence of several genes on the SRF transcription factor.

Discussion

SRF is an ancient transcription factor that directs the expression of distinct gene sets involved in growth and muscle differentiation (1, 2, 17, 18). Using the SM22α promoter, we have limited the genetic inactivation of SRF to the heart and vascular system of mice. These mice develop normally up to e8.5, at which time the SM22α-Cre transgene is activated. Thereafter, a progressive decrease in the number of SRF-expressing cardiomyocytes and aortic SMC is observed, followed by a loss in CArG-containing gene expression. The complete loss in expression of CArG-containing genes appears to follow abnormal cardiac trabecu-

DEVELOPMENTAL BIOLOGY

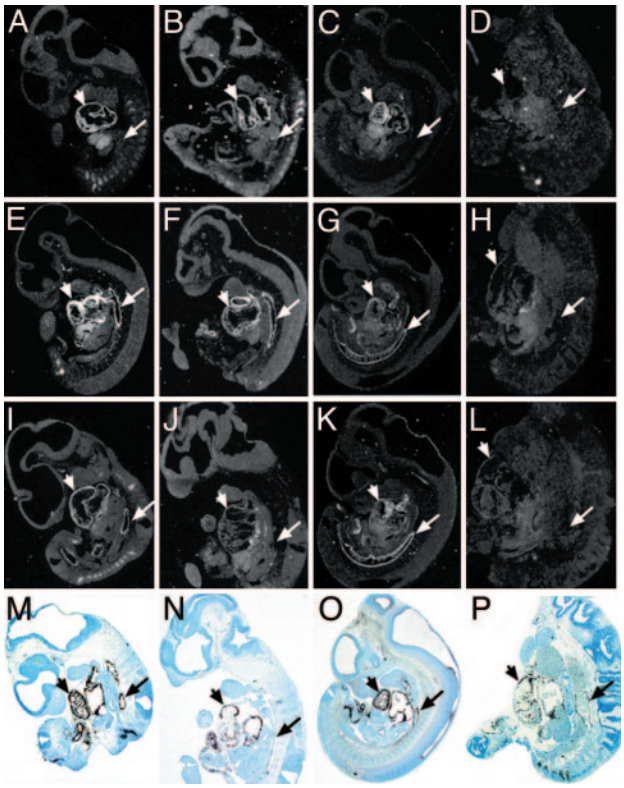

Fig. 6. ISH and immunohistochemistry of cardiac/SMC markers. e10.5 (*A*, *B*, *E*, *F*, *I*, *J*, *M*, and *N*) and e11.5 (*C*, *D*, *G*, *H*, *K*, *L*, *O*, and *P*) embryos assayed for cardiac α actin (*A–D*), SM22α (*E–H*), SMA (*I–L*) mRNA, or SMA protein (*M–P*) are shown. Wild-type embryos (*A*, *C*, *E*, *G*, *I*, *K*, *M*, and *O*) show expression of markers in heart and aorta. Mutants at e10.5 show reduced transcripts to cardiac α actin (*B*), SM22α (*F*), and SMA (*J*), which are all absent at e11.5 (*D*, *H*, and *L*). Note persistent expression of SMA protein in heart and aorta of mutant at e11.5 (*P*). Small arrows indicate heart, and larger arrows indicate aorta.

lation, an attenuated compact zone, and reduced vascular SMC recruitment to the dorsal aorta. At the ultrastructure level, SRF mutants exhibit disorganized cardiac sarcomeres and Z disks as well as loss of cortical actin/intermediate filament bundles in vascular SMC. These expression and morphological defects are followed by embryonic lethality at ≈e11.5. Collectively, these results are consistent with a model wherein mutant mice succumb to death via cardiovascular failure due to perturbations in normal muscle cytoarchitecture and contractile assembly.

SRF and Heart Development. Recently, a heart-specific Cre allele (driven by the cardiac β myosin heavy chain promoter) was used to knockout SRF in the developing heart (9). Despite the presence of a truncated SRF protein, these authors also demonstrated a marked reduction in trabeculation without measurable changes in cardiomyocyte growth and apoptosis up to e10.5, after which lethality occurred. Several cardiac transcription factors were reported to be down-regulated at e9.5 in the absence of SRF, leading the authors to speculate that SRF was a global regulator of multiple developmental genes (9). Although we also have observed variable decreases in the expression of such genes (Fig. 5), we believe this to be largely an indirect effect without consequence for the observed phenotype, because gene ablation studies of these factors do not result in myofibrillar disarray (19, 20, 21). Instead, we favor the model wherein lack of SRF results in compromised expression of numerous CArG-containing structural and signaling genes whose expression is requisite for normal embryonic cardiac function.

Indeed, the most striking aspect of the cardiac phenotype reported here is an apparent failure to assemble myosin and actin filaments into repeating units of sarcomeres. A deficiency in myofilament assembly likely leads to inefficient cardiac contraction to meet the nutritive needs of a growing embryo. Failure to assemble sarcomeres has been reported in mice lacking erythrocyte tropomodulin and p130^{Cas} (22, 23). In this context, an important structural organizing center of the mature sarcomere is the Z disk, which was itself in disarray in mutant mice. The Z disk comprises dozens of proteins (including p130^{Cas}) that act to stabilize and organize myofilaments within and among sarcomeres, couple sarcomeres to cytoskeleton and sarcoplasmic reticulum, and transduce signals to the nucleus (24). Several Z disk proteins are encoded by known (e.g., desmin and dystrophin) or hypothesized (J.M.M, unpublished work) SRF target genes. Defective expression in these and other proteins likely underlies the observed ultrastructural defect at the Z disk. Consistent with a defect in sarcomere assembly and function, we have found that neonatal cardiomyocytes lacking SRF show significantly diminished α-actinin and α-tropomyosin (R.O.B. and R.P.M., unpublished work).

Myofibrillar disorganization and irregular heartbeat have been reported in mice lacking the SRF-dependent gene *NCX1*, which is involved in calcium transport through the sarcoplasmic reticulum (25). Given the *NCX1* mRNA expression data reported here (Fig. 5), the cardiac phenotype observed in the absence of SRF may also relate to decreases in this important regulator of cardiac function. Finally, it is likely that decreases in expression of cardiac thick and thin filaments (Fig. 5) contribute to the ultrastructure defects seen at the cardiac sarcomere in SRF mutant hearts. Based on these results, we propose SRF-deficient mice exhibit heart failure due to defective SRF target gene expression, the protein products of which coordinate Z disk formation, sarcomeric assembly, and signaling leading to normal acto-myosin coupling.

SRF and Vascular SMC Development. Functional circulation reaches a steady state at e10.0–e10.5 days of gestation in the mouse (26). This embryonic period is pivotal for normal cardiovascular development, as evidenced by the ever-increasing number of lethal phenotypes that are linked to the heart and blood vessels at this time point (http://research.bmn.com/mkmd). One major SMC-restricted gene that is normally expressed at this time is SM myosin heavy chain (27). We do not detect this transcript in SMC of the dorsal aorta of mutant mice, and extensive ultrastructural analysis reveals no evidence of thick filaments in vascular SMC. Moreover, despite the expression of SMA protein in the dorsal aorta, zones of actin/intermediate filament bundles are not present in these cells.

We also observed a significant reduction in the recruitment of cells to the dorsal aspect of the aorta. Previous studies in embryonic stem cells null for SRF showed defects in cell migration, presumably as a result of a disrupted cytoskeleton (6). Interestingly, flies and social amoeba null for SRF also display defects in cell migration that are thought to be a result of an altered cytoskeleton (5, 28). These results point to a pivotal and ancient role for SRF in normal cytoarchitecture, the disruption of which has consequences for both life form and function. In the present context, the reduction in SMC recruitment to the dorsal aorta could have deleterious effects on functional circulation in the embryo. Taken together, our data suggest that the absence of SRF in vascular SMC may impair the ability of such cells to propagate a pressure wave front generated from the heart. However, given the concurrent cardiac defects, we cannot at this time discriminate between death from cardiac dysfunction and death from vascular insufficiency. Inactivating SRF with a more specific SMC promoter-driven Cre (29, 30) should clarify this important issue.

A large fraction of known SRF-dependent target genes is restricted to SMC (2). Evidence implicating SRF in the control of SMC CArG genes is limited to *in vitro* and *in vivo* transgenic reporter assays (2, 7). The data reported here provide genetic support for SRF-regulating SMC CArG genes *in vivo*. However, definitive proof for direct involvement of SRF in such gene expression will require the mutation of SMC CArG elements in their native genomic context.

Perspective

Whereas other transcription factors have paralogs functioning in a context- or cell-restricted manner, SRF is a widely expressed single-copy gene with no known paralogs. SRF must therefore selectively activate cell- and context-specific programs of gene expression through the recruitment of coactivators (31). One such SRF-associated coactivator is myocardin (MYCD) (32). MYCD stimulates SMC and cardiac CArG-dependent gene expression (32–36), and its inactivation in mice leads to embryonic death at e10.5 due to defects in vascular SMC differentiation (21). Interestingly, no changes in cardiac development or cardiac SRF-dependent gene expression were evident in MYCD-null mice, supporting the concept of compensatory pathways for these processes to occur in the heart without MYCD. That SRF inactivation leads to both cardiac and vascular SMC defects underscores its essential role in the coordinate expression of genes necessary for the normal development and function of these cell types. A major goal, therefore, will be to define the full complement of genes regulated directly by SRF (the CArGome) and elucidate their function in heart and vascular development.

J.M.M. thanks Alexander and Erika Miano, Jeffrey R. Bentley for assistance with the EM graphics, and Jeffrey W. Streb and Dr. James Palis for stimulating scientific exchange. We thank Dr. Robert J. Schwartz for kindly communicating his laboratory's results before publication. This work was supported by National Institutes of Health Grants HL-62572 (to J.M.M.); HL-67272 (to R.P.M.), HL-60655 (to H.W.), and NS34814 (to D.D.G., an Investigator of the Howard Hughes Medical Institute). N.R. is a Damon Runyon Fellow of the Damon Runyon Cancer Research Foundation (DRG#1733-02).

1. Johansen, F. E. & Prywes, R. (1995) *Biochim. Biophys. Acta* **1242,** 1–10.
2. Miano, J. M. (2003) *J. Mol. Cell. Cardiol.* **35,** 577–593.
3. Escalante, R. & Sastre, L. (1998) *Development (Cambridge, U.K.)* **125,** 3801–3808.
4. Fraser, A. G., Kamath, R. S., Zipperlen, P., Martinez-Campos, M., Sohrmann, M. & Ahringer, J. (2000) *Nature* **408,** 325–330.
5. Guillemin, K., Groppe, J., Dücker, K., Treisman, R., Hafen, E., Affolter, M. & Krasnow, M. A. (1996) *Development (Cambridge, U.K.)* **122,** 1353–1362.
6. Schratt, G., Philippar, U., Berger, J., Schwarz, H., Heidenreich, O. & Nordheim, A. (2002) *J. Cell Biol.* **156,** 737–750.
7. Owens, G. K., Kumar, M. S. & Wamhoff, B. R. (2004) *Physiol. Rev.* **84,** 767–801.
8. Arsenian, S., Weinhold, B., Oelgeschlager, M., Ruther, U. & Nordheim, A. (1998) *EMBO J.* **17,** 6289–6299.
9. Parlakian, A., Tuil, D., Hamard, G., Tavernier, G., Hentzen, D., Concordet, J.-P., Paulin, D., Li, Z. & Daegelen, D. (2004) *Mol. Cell. Biol.* **24,** 5281–5289.
10. Spencer, J. A. & Misra, R. P. (1996) *J. Biol. Chem.* **271,** 16535–16543.
11. Nelson, T. J., Duncan, S. A. & Misra, R. P. (2004) *Circ. Res.* **94,** 1059–1066.
12. Soriano, P. (1999) *Nat. Genet.* **21,** 70–71.
13. Miano, J. M. & Olson, E. N. (1996) *J. Biol. Chem.* **271,** 7095–7103.
14. Li, L., Miano, J. M., Mercer, B. & Olson, E. N. (1996) *J. Cell Biol.* **132,** 849–859.
15. Kim, S., Ip, H. S., Lu, M. M., Clendenin, C. & Parmacek, M. S. (1997) *Mol. Cell. Biol.* **17,** 2266–2278.
16. Croissant, J. D., Kim, J. H., Eichele, G., Goering, L., Lough, J., Prywes, R. & Schwartz, R. J. (1996) *Dev. Biol.* **177,** 250–264.
17. Camoretti-Mercado, B., Dulin, N. O. & Solway, J. (2003) *Resp. Physiol. Neurobiol.* **137,** 223–235.
18. Chai, J. & Tarnawski, A. S. (2002) *J. Physiol. Pharmacol.* **53,** 147–157.
19. Molkentin, J. D., Lin, Q., Duncan, S. A. & Olson, E. N. (1997) *Genes Dev.* **15,** 1061–1072.
20. Lyons, I., Parsons, L. M., Hartley, L., Li, R., Andrews, J. E., Robb, L. & Harvey, R. P. (1995) *Genes Dev.* **9,** 1654–1666.
21. Li, S., Wang, D.-Z., Richardson, J. A. & Olson, E. N. (2003) *Proc. Natl. Acad. Sci. USA* **100,** 9366–9370.
22. Honda, H., Oda, H., Nakamoto, T., Honda, Z., Sakai, R., Suzuki, T., Saito, T., Nakamura, K., Nakao, K., Ishikawa, T., *et al.* (1998) *Nat. Genet.* **19,** 361–365.
23. Chu, X., Chen, J., Reedy, M. C., Vera, C., Sung, K.-L. P. & Sung, L. A. (2003) *Am. J. Physiol.* **284,** H1827–H1838.
24. Pyle, W. G. & Solaro, R. J. (2004) *Circ. Res.* **94,** 296–305.
25. Koushik, S. V., Wang, J., Rogers, R., Moskophidis, D., Lambert, N. A., Creazzo, T. L. & Conway, S. J. (2001) *FASEB J.* **15,** 1209–1211.
26. McGrath, K. E., Koniski, A. D., Malik, J. & Palis, J. (2003) *Blood* **101,** 1669–1676.
27. Miano, J. M., Cserjesi, P., Ligon, K. L., Periasamy, M. & Olson, E. N. (1994) *Circ. Res.* **75,** 803–812.
28. Escalante, R., Yamada, Y., Cotter, D., Sastre, L. & Sameshima, M. (2004) *Mech. Dev.* **121,** 51–56.
29. Regan, C. P., Manabe, I. & Owens, G. K. (2000) *Circ. Res.* **87,** 363–369.
30. Kühbander, S., Brummer, S., Metzger, D., Chambon, P., Hofmann, F. & Feil, R. (2000) *Genesis* **28,** 15–22.
31. Wang, Z., Wang, D.-Z., Hockemeyer, D., McNally, J., Nordheim, A. & Olson, E. N. (2004) *Nature* **428,** 185–189.
32. Wang, D.-Z., Chang, P. S., Wang, Z., Sutherland, L., Richardson, J. A., Small, E., Krieg, P. A. & Olson, E. N. (2001) *Cell* **105,** 851–862.
33. Chen, J., Kitchen, C. M., Streb, J. W. & Miano, J. M. (2002) *J. Mol. Cell. Cardiol.* **34,** 1345–1356.
34. Du, K., Ip, H. S., Li, J., Chen, M., Dandre, F., Yu, W., Lu, M. M., Owens, G. K. & Parmacek, M. S. (2003) *Mol. Cell. Biol.* **23,** 2425–2437.
35. Yoshida, T., Sinha, S., Dandre, F., Wamhoff, B. R., Hoofnagle, M. H., Kremer, B. E., Wang, D.-Z., Olson, E. N. & Owens, G. K. (2003) *Circ. Res.* **92,** 856–864.
36. Wang, Z., Wang, D.-Z., Pipes, G. C. T. & Olson, E. N. (2003) *Proc. Natl. Acad. Sci. USA* **100,** 7129–7134.